Particle Size Dependence of MnO Reduction for Fabrication of Al − $AlMnO_X$ Composite vir Stir Casting

Khalid Almadhoni[1], Sabah Khan[2]

[1]Dr. Engineer, Department of Mechanical Engineering, Faculty of Engineering, Sabratha University, Sabratha, (Libya)

[2] Dr. Assistant Prof., Department of Mechanical Engineering, Faculty of Engineering and Technology, JMI, Jamia Nagar, New Delhi-110025 (India)

DOI: https://doi.org/10.21467/proceedings.4.21

* Corresponding author email: K_almadhoni@yahoo.com

ABSTRACT

In the present work, a composite of Al matrix reinforced with 10% MnO particles has been developed using stir casting technique. MnO with particles size of range of 53 to 90 μm for composite (A) and 188 to 250 μm for composite (B) as reinforcement and pure Mg powder as wetting agent to improve the wettability of MnO particulates with molten Al were used for production of Al-MnO composites having 10 wt.% of MnO. The pouring temperature and stirring speed have been set to 750 ℃ and 900 RPM, respectively. The main purpose of this work is to study the dependence of MnO reduction on particle size for fabrication of Al matrix composite via stir casting route. For structural analysis, fundamental material characterization like SEM, EDX, XRD and OM was carried out for developed composite samples. The results reveal that an in-situ formed finer alumina (Al_2O_3) particles and an intermetallic precipitate of Al-Mn as a result of chemical reaction between molten Al and MnO particles have been observed using SEM with EDX of both developed composite samples. SEM with EDX analysis has detected that the composition of reinforcement particles of composite sample of A contains Al and O, which indicates presence of in-situ generated Al_2O_3. While the composition of reinforcement particles of composite samples of B contains high percentage of Mn, high percentage of O and low percentage of Al, which indicates presence of unreacted MnO and generated in-situ Al_2O_3 to form in-situ ($AlMnO_x$) intermediate compound. This has been also confirmed by elemental mapping SEM analysis. SEM analysis of in-situ $AlMnO_x$ particles at high magnification has detected that their structure is porous. Optical micrographs have shown that a good bonding between particles and the matrix in both developed composite samples with presence some aggregations of particles and pores. For both developed composite samples, the amount of (Al-Mn) phases formed in the specimens may be too little to be detected directly from the bulk specimens by XRD. Phase identification by X-ray diffraction technique verifies of presence Al and Al_2O_3 phases in composite sample of A, while it verifies of presence Al and MnO phases in composite sample of B.

Keywords: Al, MnO, Morphology, microstructure, $AlMnO_x$, Al-Matrix Composite.

 ISBN: 978-81-936820-6-7

1 Introduction

The low density, environment resistance and adequate mechanical and physical properties of Al metal matrix composites (AMMC's) make them one of the most interesting material alternatives for the manufacture of lightweight parts for many types of modern engineering equipments.. Composites are classified by matrix into metal matrix composites (MMC's), ceramic matrix composites (MMC's) and polymer matrix composites (MMC's) while by filler type are classified into particle reinforced composite, fiber reinforced composites and structural composites [1-2], Figure 1.1.

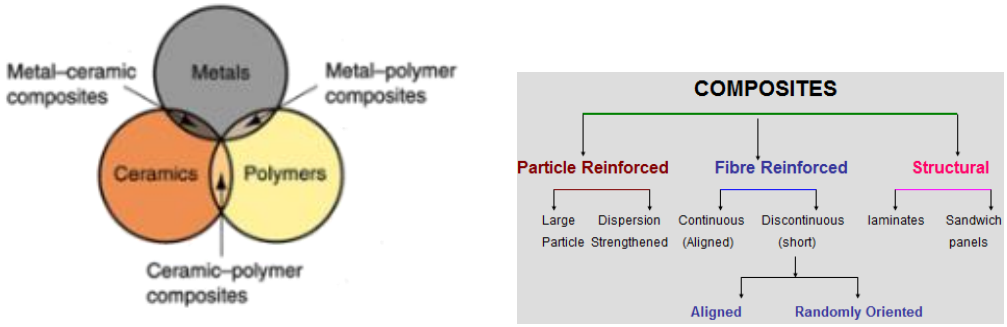

(a) (b)

Figure 1.1: Classification of composites (a): by matrix type and (b): by filler type (1-2)

Al and its alloy are the most commonly used metal matrix materials in the production of MMC's because of their preferred properties such as lightness, corrosion resistance and ductility and easy availability. Reinforcing of AMC with whiskers, short fibers or particulates of various kinds of ceramic materials such as SiC, SiO_2, Al_2O_3, MgO, ZnO, BeO, MnO_2, TiO_2, TiC, etc., provide properties compared to monolithic base alloy [3]. MMC's as compared to other MMCs have superior values of refractoriness, compressive strength, hardness and show excellent wear resistance [2-4-5]. Thermal characterization is one of the prime physical characterization of composites, which also include electrical, magnetic and optical properties. Heat is transferred at a higher rate across materials of high thermal conductivity than across materials of low thermal conductivity [6]. Melt stir casting has a good potential in all-purpose applications as it is a low cost MMC's production method. Its advantages lie in its simplicity, flexibility and applicability to large quantity production. This route is also attractive because, in principle, it allows a conventional metal processing method to be used, and hence reduces the final cost of the product [7-8]. The particle size and orientation have greater effect on the properties of the composite. Zhou et al. [9] used Al_2O_3 with different size to fill silicone rubber, and reported that nano-sized Al2O3 composite exhibited higher thermal conductivity and mechanical properties than the micro-sized one. Many researchers have reported that at the same percentage of reinforcement, smaller particle size leads to lower inter-particle distance and more chances for the formation of thermal conductive 'pathway' [10]. When the average inter-particle distance is in a suitable range, extensive plastic deformation in the matrix

ISBN: 978-81-936820-6-7
Proceedings DOI: 10.21467/proceedings.4

Series: AIJR Proceedings

can be easily induced [11–12]. Operating temperature should be kept at semisolid stage to improve the wettability of reinforcements with the matrix, this is attributed to interactions among the particles themselves, between solid Al and particles and between remaining liquid phases of Al with particles [13]. Manganese has been known as an alloying element of Al alloys which contributes to uniform deformation. The effect of Mn on the mechanical behavior of Al alloys is investigated by S. W. Nam and D. H. Lee. It was found that as the Mn content increases over 0.5 wt% in Al alloys, both yield and ultimate tensile strength increased significantly without reduction of ductility. Adding Mn to aluminum alloys also improves both low-cycle fatigue resistance and corrosion resistance [14]. Release of manganese (Mn) in the matrix, intermetallic compound of Al-Mn precipitated in the matrix in different phases. Results showed that the porosity was evident in the micrographs and with increase in Al_2O_3-MnO_2 wt%, the strength improved and the ductility decreased [15]. Adding Mg improves the wettability of MnO_2 with molten Al and thus increases the amount of reinforcing phase in the composite material [16]. A. Agarwal, S. Singh and others prepared hybrid composites using both in-situ and ex-situ approaches together by dispersing powder mixture of alumina (Al_2O_3) and manganese dioxide (MnO_2) in a ratio of 1:1 but with different sizes, by stir casting method in Al matrix. They investigated and compared the microstructures and mechanical properties of Al-Al_2O_3, Al-MnO_2 and Al-Al_2O_3(MnO_2) composites. Results showed that fine Al_2O_3 particles were formed as result of reduction of MnO_2 by Al and Mn was released in the matrix, which combined with Al to form intermetallic compounds of Al-Mn precipitate in the matrix in different phases of Al-Mn and reinforce it. It was also found that with increase in wt.% of Al_2O_3- MnO_2, mechanical properties of the composite enhanced with decrease in ductility, however they reported evidence of porosity in the micrographs [17].

2 Manganese Oxide Mesoporous Solids (MOMS)

As we know mesoporous material contain pores with diameters between 2 and 50 nm. These materials are classified into according to their size by IUPAC. The microporous materials have pore diameters of less than 2 nm and macroporous materials have pore diameters of greater than 50 nm; the mesoporous category thus lies in the middle. Manganese oxide mesoporous solids (MOMS) are gaining popularity and are characterized by a high surface area mesoporous and /or microporous mixed oxidic solid [16]. Researchers have found that the surface area of Al$x$$MnO_2$ is 711 m^2/g, while the mean pore diameter was 3.6 nm. Results showed that the extreme surface area value of Al$x$$MnO_2$ is attributed to the existence of an open network interconnected particles forming features medium height with no preferential orientation [18].

3 Material Selection

The composite of Al-AlMnOX was fabricated by stir casting method. Pure aluminum (AA-1070) with 99.77% purity is used as the matrix for fabrication of the composite. Table 3.1 gives the chemical composition of the matrix

Table 3.1 Chemical composition of Matrix Al (wt %)

Si%	Cu%	Mg%	Fe%	Zn%	Ni%	Mn%
0.0637	0.0152	0.0017	0.0874	0.0130	0.0056	0.0026
Cr%	V%	Ti%	Sn%	Bi%	Pb%	Al%
0.0024	0.0105	0.0071	0.0033	0.0023	0.0040	99.77

Manganese (II) oxide, also called Manganese monoxide, is used as reinforced material, in the particle size range of 53 to 90 µm for composite (A) and 188 to 250 µm for composite (B) and with 10% RVR. The purity of the powder, its density and the size of the particles selected for the present l study is given in the Table 3.2.

Table 3.2: Specifications of MnO powder selected for present study

Purity %	Density (g/mL) at 25 °C(lit.)	Size of particles selected
99	5.45	(188-250) microns
99	5.45	(53-90) microns

Additive material:

Pure Mg powder was used 1% by weight as wetting agent to increase the wettability of MnO particulates with molten Al. Mg is added to in order to help wetting of particles in molten Al and to retain the particles inside the melt [19-20].

4 Experimental Setup and Fabrication of Composite

The experimental setup consist of conical shaped silicon carbide (SiC) crucible for melting of Al, as it withstands high temperature up to [1700°C]. The crucible is placed in electric melting furnace made up of high ceramic alumina around which heating element is wound. The coil which acts as heating element is K thermocouple (Nickel-Chromium / Nickel-Alumel). Due to the high affinity of Al at liquid stage to react with atmospheric oxygen, the process of stirring is carried out in closed chamber with an inert gas such as nitrogen or argon. Closed chamber is formed. Due to corrosion resistance to atmosphere, silver steel is selected as stirrer shaft material. One end of shaft is connected to 0.05 HP motor, while at the other end blades are welded. Four blades are welded to the shaft at 90°C. The speed can be varied from (0 - 4000) RPM. A permanent mould made of cast iron used to pour the fabricated composite. Figure 4.1 shows a setup of stir casting apparatus developed in the lab.

Figure 4.1: Stir-Casting-Apparatus Set-up

ISBN: 978-81-936820-6-7
Proceedings DOI: 10.21467/proceedings.4

Series: AIJR Proceedings

The impurities and thick oxide layers on the surface are removed by mechanical cleaning by grinding on grinding belt machine, polishing on polishing machine followed by chemical etching by immersing the part in 50% nitric acid aqueous solution at room temperature for 15 min. The part is then rinsed in cold water, followed by hot water and blow dried, as suggested by R. Gadag, 2010 and G. Totten, 2003 [21-22] .The procedure of preparing the composite was carried out by initially setting the temperature at 500°C and then gradually increasing up to 850°C. The pure Al (purity 99.77 %) matrix was cleaned to remove impurities, weighed and then kept in the crucible for melting. Nitrogen gas was used as inert gas to avoid oxidation. Required quantities of 1% pure Mg powder as wetting agent and 10% MnO as reinforcement particles in the size of range of 53 to 90 μm for composite (A) and 188 to 250 μm for composite (B) are weighed to be added. In order to remove any gases and moisture present in reinforcing material, MnO is preheated for half an hour at temperature of 200°C [19-20]. After the matrix completely melts, it was stirred for one minute for homogeneity. Temperature is set to 630°C which is below the melting temperature of the matrix. While stirring semisolid Al, a preheated the wetting agent Mg is added followed by preheated particulate MnO. Dispersion of preheated reinforcements at the semisolid stage of the matrix enhances the wettability of the reinforcement, thus preventing the particles from settling at the bottom of the crucible [23]. Measured flow rate of reinforcements was about 0.2 gm/s. Dispersion time was taken as 4 minutes. Stirrer rpm is gradually increased from 0 to 900 RPM with the help of speed controller. Immediately, after completion of dispersion of particles with continued stirring at semisolid stage, slurry was reheated up to 750°C to make sure slurry is fully liquid. Total stirring time was 8 minutes. Composite slurry was poured in a cast iron preheated mold. Preheating of mold at 500°C was done to remove the entrapped gases from the mold which could reduce the porosity and improve the mechanical properties of composite [20].

4 Results

The specimen were removed from the mold and taken for morphological characterization. The morphological studies of the composite were carried out using the following techniques:

4.1 Scanning Electron Microscopy (SEM/EDX)

The morphology of the composite was observed by scanning electron microscopy (SEM),using a SEM-EDX Oxford INCA 400 model at an acceleration voltage 10 kv. The micrographs were taken at a magnification of 1000.

Composite A:

Figure 5.1 (a) shows un-etched SEM micrograph of Al-10wt.%MnO composite A at 600X and its chemical composition of entire area is given in Figure 5.1 (b) at an encircled spot by EDX analysis. Figure 5.1 (a) indicates white string phase. It also shows dark gray phase.

These phases are identified as Al and O, as well as a virtually non-existent ratio of Mn by EDX in Figure 5.1 (b).

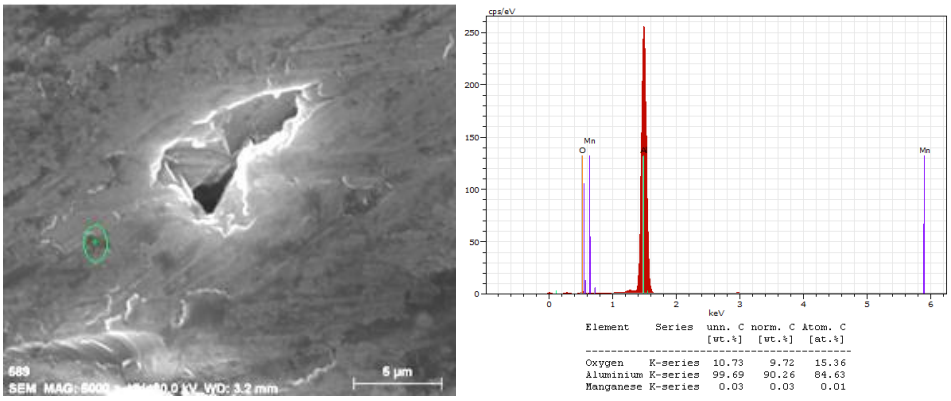

(a) (b)

Figure 5.1: (a) Un-etched SEM micrograph of Al-10wt.%MnO composite A at 600X and (b) composition of encircled spot by EDX

Presence of Mn traces in the Al-matrix is attributed to the result of the reduction of MnO with Al melt. Mn released in the matrix reacts with Al-rich matrix to make Al_2O_3 and an intermetallic precipitate of Al-Mn as is suggested by the following chemical reaction taking place in the (Al-MnO) composite system: Figure 5.3 (a) indicates SEM micrograph of the Al-10wt.%MnO composite B at 600X and its chemical composition is given in Figure 5.3 (b) at a encircled spot by EDX analysis.

$2Al + 3MnO = 3Mn + Al_2O_3$ (1),

$Al+Mn = AL(Mn)$ ppt. (2).

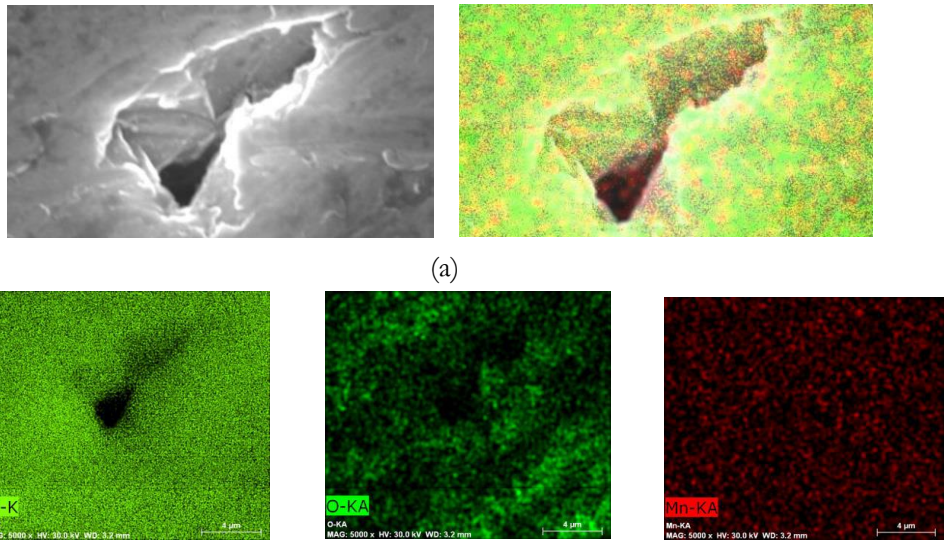

(a)

(b)

Figure 5.2: Un-etched elemental mapping SEM micrograph (Al, O and Mn) of Al-10wt.%-MnO composite A at 5000X. at 300X, (a) Collectively and (b) Separately

ISBN: 978-81-936820-6-7
Proceedings DOI: 10.21467/proceedings.4

Series: AIJR Proceedings

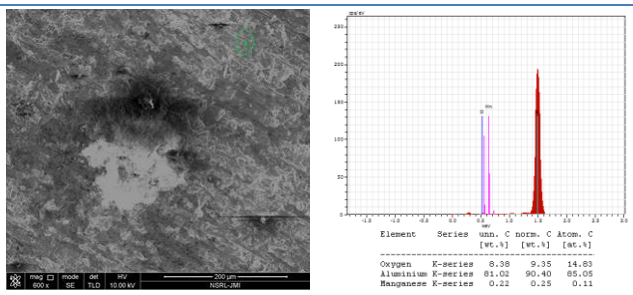

(a) (b)

Figure 5.3: (a) Un-etched SEM micrograph of Al-10wt.%MnO composite B at 600X and (b) composition of encircled spot by EDX.

Figure 5.3 (a) indicates fine bright particles in the Al matrix identified as Al_2O_3 particles by EDX in Figure 5.3 (b) and traces of Mn is detected by EDX which indicates presence of Mn in the Al matrix to make an intermetallic precipitate of Al-Mn. Presence of Al_2O_3 and Al-Mn is attributed to the result of the chemical reaction between Mn released in matrix by reduction of MnO with molten Al and Al-rich matrix itself in the composite system as is suggested by the reactions referred to in equations (1) and (2).

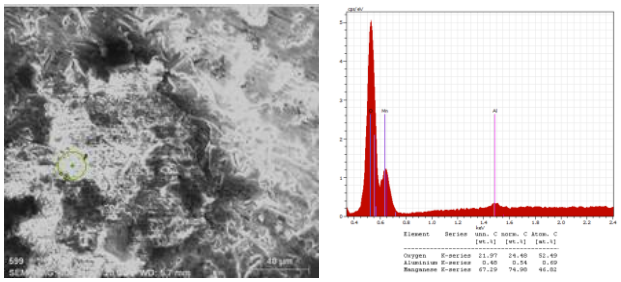

(a) (b)

Figure 5.4: (a) Un-etched SEM micrograph of Al-10wt.%MnO composite B at 600X and (b) composition of encircled spot by EDX

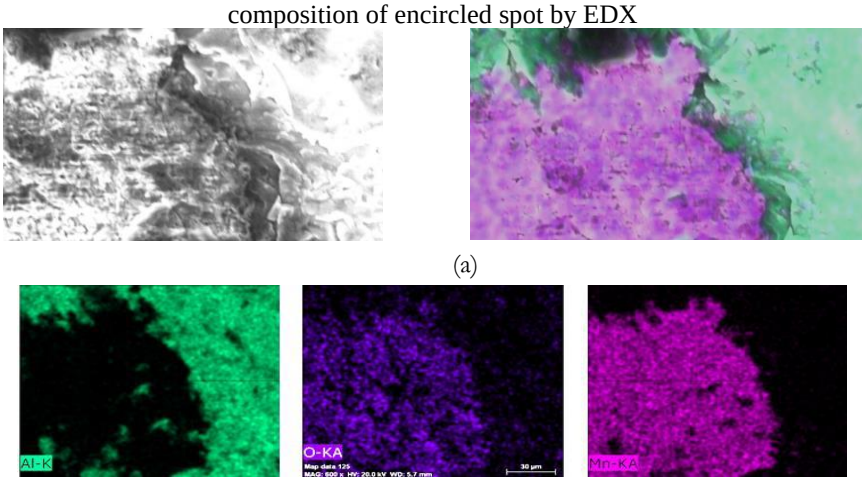

(a)

(b)

Figure 5.5: Un-etched elemental mapping SEM micrograph (Al,O and Mn) of Al-10wt.%-MnO composite B at 600X, (a) Collectively and (b) Separately

Figure 5.4 (a) shows un-etched SEM micrograph of the reinforcement particle in the matrix of composite B at 600X and its chemical composition is recorded by EDX in Figure 5.4 (b). EDX analysis indicates presence of Mn in the Al matrix to make an intermetallic precipitate of Al-Mn.

Figure 5.5 illustrates un-etched elemental mapping SEM micrograph (Al, O and Mn) of composite B at 600X. Figure 5.9 (a) illustrates presence of Al (green), O (cyan) and Mn (Pink) collectively in the matrix. More O and Mn with little Al are seen to form porous AlMnOx particle, thus confirming Al_2O_3 (light green) embedded in an unreacted MnO particle (light pink) in the Al-matrix (green). More O at the matrix-reinforcement boundary is clearly visible to appear as dark green Al_2O_3 layer from matrix side and dark pink MnO layer from reinforcement side. Distribution of Al, O and Mn is shown in Figure 5.5 (b) separately, thereby confirming what has been indicated in Figure 5.5 (a).

4.2 Optical Microscopy

Optical microscopic technique was applied for the analysis of microstructure of the composite samples. The magnified images of the samples were obtained using a microscope digital camera Leica DM 2500 M. Optical images of composites were taken at different points of the samples surfaces. All of the analyses were carried out at room temperature. The maximum magnification obtained with the optical microscope was about 500X.

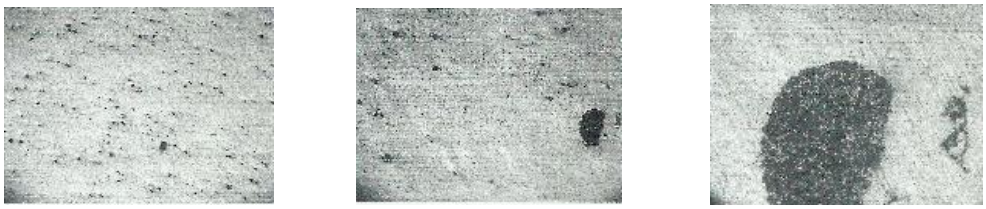

(a) (b) (c)

Figure 5.6: Un-etched OM of Al-10wt.%MnO composite A at (a): 25X, (b): 100X and (c): 500X

On macroscopic scale at low magnification, at 25X in Figure 5.6 (a), un-etched optical micrograph of Al-10wt.%MnO composite A is shown. The density of small dark spots in the matrix is less than those observed in composite samples of A. In Figure 5.6 (b) at higher magnification of 100X, few small light spots are inside the bigger particles. Figure 5.6 (c) at higher magnification of 500X indicates big reinforcement particle containing more small light spots than those indicated in composite samples of A1, which may indicate formation of porous alumina (Al_2O_3) particle or agglomerated cluster of alumina particles. It also shows a good bonding between the particles and matrix.

ISBN: 978-81-936820-6-7
Proceedings DOI: 10.21467/proceedings.4

Series: AIJR Proceedings

(a) (b) (c)

Figure 5.7: Un-etched OM of Al-10wt.%MnO composite B at (a): 25X, (b): 100X and (c): 500X.

Figure 5.7 (a) shows un-etched optical micrograph of Al-10wt.%MnO composite B at 25X. It indicates reinforcement particles surrounded by small dark spots in the matrix. Small light and dark spots are inside the bigger particles are visible in Figure 5.7 (b) at higher magnification of 100X, which could be pores and in-situ formed Al_2O_3 particles embedded in MnO particles. It also shows an aggregation of the particles. On microscopic scale, at magnification of 500X in Figure 5.7 (c), big aggregated reinforcement particles containing small light and dark spots is shown. This could be indication of in-situ formed alumina particles embedded in MnO particles to form porous in-situ generated intermediate compound (AlMnOX) particle. It also shows a good bonding between the particle and matrix.

4.3 X-ray diffraction (XRD)

XRD analysis is based on constructive interference of monochromatic X-rays and a material sample. The characteristic x-ray diffraction pattern generated in the XRD analysis provides a unique "fingerprint" of the crystals present in the sample. In the present analysis as part of morphological characterization, a comparative XRD analysis is carried out between the Matrix Al and the developed composite.

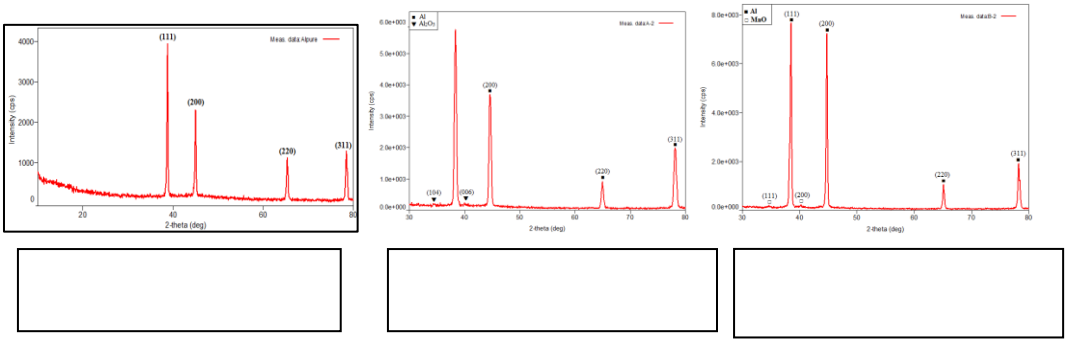

The Figure 5.8 illustrates the XRD result of the matrix (Al). The result reveals that the main phases present belong to Al, which is present in the form of phases e.g.,Al(111), Al(200), Al(220) and Al(311). The Figure 5.9 illustrates the XRD result of developed Al-10%MnO composite A. The result shows that the main phases present belong to Al (largest peaks) and Al_2O_3 (lower peaks). The Al is present in the form of phases i.e. Al (111), Al (200), Al (220)

and Al (311), while Al_2O_3 is present only in the form of phases i.e. Al_2O_3 (104) and Al_2O_3 (006) phases. Peaks are identified by using JCPDS software. The peak intensities of Al in the manufactured composite are changed. There is a significant increase in peak intensities of Al (111) and Al (200) phases, and slight increase in peak intensity of Al (311) phase. However, the peaks are of only of Al and Al_2O_3 phases, which confirms that MnO particles have been completely reduced with molten Al forming in-situ Al_2O_3 particles and little amount of an intermetallic (Al-Mn) compound phases that can be detected directly from the bulk specimen as indicated by XRD. The Figure 5.10 illustrates the XRD result of developed Al-10%MnO composite B. The result shows that the main phases present are Al (largest peaks) and MnO (lower peaks). The Al is present in the form of phases i.e. Al(111), Al(200), Al(220) and Al(311). MnO is present in the form MnO(111) and MnO(200). Peaks are identified by using JCPDS software. The peak intensities of Al in the manufactured composite are changed. There is a significant increase in peak intensities of Al(111) and Al(200) phases, and moderate increase in peak intensity of Al(331). Manganese oxide was indicated in low intensities of MnO(111) and MnO(200) phases. However, there are peaks corresponding to Al and MnO phases. This confirms that MnO particles have been partially reduced with molten Al forming little amount of in-situ Al_2O_3 particles and an intermetallic (Al-Mn) compound phases to be detected directly from the bulk specimen as indicated by XRD.

6 Conclusion

Results show that the use of manganese oxide (MnO) as reinforcing ceramic particles in pure aluminum can produce (Al-Al_2O_3) or (Al-$AlMnO_X$) in-situ particulate composite via stir casting method. The composite can be developed by controlling the particle size. There is appreciable reaction between MnO particles and melted Al matrix, producing in-situ finer Al_2O_3 particles and an intermetallic precipitate of Al-Mn compound, which could be in various phases with uniform distribution in Al to make Al-alloy as matrix. Some portion of Al diffuses into MnO particles to react with oxygen and generate Al_2O_3 particles forming MnO porous intermediate compound ($AlMnO_X$). Fine alumina (Al_2O_3) particles and an intermetallic precipitate of Al-Mn as a result of chemical reaction between molten Al and manganese oxide (MnO) particles have been observed using scanning electron microscopy (SEM) with energy dispersive X-ray analysis (EDX) of entire area of both developed composite samples. EDX analysis of the reinforcement particles of developed composite sample B has detected that their composition contains high percentage of Manganese (Mn) and Oxygen (O) with low percentage of Al, which indicates presence of unreacted MnO and generated Al_2O_3 particles. SEM analysis of in-situ formed $AlMnO_X$ particles at high magnification has detected a characterized porous structure. EDX Analysis of the reinforcement particles of composite sample of A has detected that their composition contains high percentage of (Al) and (O) without presence of (Mn), which indicates presence of generated Al_2O_3 only. This has been also confirmed by elemental mapping SEM analysis.

ISBN: 978-81-936820-6-7

Series: AIJR Proceedings
Proceedings DOI: 10.21467/proceedings.4

Optical micrographs have indicated presence of porosities in the both composite samples, but their density varies from A to B, depending on the reinforcement particles size. Optical micrographs have shown that a good bonding between particles and the matrix of both developed composite samples.

XRD analysis has indicated that the main phases present in both developed composite samples are Al (largest peaks). It is present in the form of phases Al(111), Al(200), Al(220) and Al(311), but with various intensities. Al_2O_3 (lower peaks) has only been indicated in composite sample of A. It is present in the form of phases Al_2O_3(104) and Al_2O_3(006). MnO (lower peaks) has been indicated in composite sample B,. It is present in the form of phases MnO(111) and MnO(200) of composite sample B. MnO phases of composite sample B have shown low intensity peaks, which indicates that less amount of unreacted MnO particles. Amount of intermetallic compound (Al-Mn) phases formed in the specimens of both developed composites may be too little to be detected directly from the bulk specimen by XRD.

Thus, the morphological structure analysis using XRD of developed composite samples indicates the presence of a porous $AlMnO_X$ embedded in pure Al matrix in developed composite sample B only.

References

[1] ASM International Handbook Committee: "Composite, Engineered Materials Handbook," Volume 1, Third Printing, August 1989.

[2] K. Surappa, "Aluminium matrix composites: Challenges and opportunities". Sadhana. 28: 319-334, 2003.

[3] Sabah Khan, "Analysis of Wear Rate and Tribological Behavior of Aluminum Cast Alloy A356 and Granite Composite at Different Speeds", (IJEAT), Volume-5, Issue-3, February 2016, Pp 128 – 131.

[4] Khedera, G. Marahleh and D. Al-Jameaa, "Strengthening of Aluminum by SiC, Al2O3 and MgO". Jordan Journal of Mechanical and Industrial Engineering. Volume 5, Number 6, Dec. 2011.

[5] D. Ramesh, R. Swamy and T. Chandrashekar, "Effect of weight percentage on mechanical properties of frit particulate reinforced Al6061 composite". ARPN Journal of Engineering and Applied Sciences. Vol. 5, No. 1, January 2010.

[6] K. Almadhoni and S. Khan," Evaluation of the effective thermal properties of aluminum metal matrix composites reinforced by ceramic particles", International journal of current engineering and technology, E-ISSN 2277 – 4106, P-ISSN 2347 – 5161, Vol.5, No.4, 2015.

[7] R. Calin, M. Pul and Z. Pehlivanli, "The Effect of Reinforcement Volume Ratio on Porosity", Materials Research, 15(6): 1057-1063, 2012.

[8] N. Jit, A. Tyagi and N. Singh, Al-Cu-Si - (Al_2O_3)p composites using A 384.1 Al Alloys.. Vol. 21, No. 10, S066-071, 2009.

[9] Zhou W. Y., Qi S. H., Tu C. C., Zhao H. Z., Wang C. F., Kou J, "Effect of the particle size of Al_2O_3 on the properties of filled heat-conductive silicone rubber" Journal of Applied Polymer Science, 104, 1312–1318 (2007).

[10] Ling W., Gu A. J., Liang G. Z., Yuan L." New composites with high thermal conductivity and low dielectric constant for microelectronic packaging", Polymer Composites, 31, 307–313 (2010).

[11] R. Gadag and A. Shetty, Handbook of engineering chemistry, Department of chemistry, National institute of technology, Karnataka, Shurathkal, 2010.

[12] J. Hashim, L. Looney and M. Hashmi, "The wettability of SiC particles by molten aluminum alloy", Journal of Materials Processing Technology, 119(1-3):324-328, 2001.

[13] K. Almadhoni and S. Khan, "Review of effective parameters of stir casting process on metallurgical properties of ceramics particulate Al composites", Journal of mechanical and civil engineering (IOSR-JMCE), Vol. 12, Issue 6, Ver. IV, PP 22-40, 2015.

[14] S. Nam and D. Lee, "The effect of Mn on the Mechanical Behavior of Al Alloys, Metals and materials", Vol. 6, No. 1, pp. 13-16, 2000.

[15] V. Tirth, "Process parameters and improvements in properties of metals and alloys by squeeze casting", IJNSTEEES, International Science Press 2, pp 26- 61, 2009.

[16] C. Singh and K. Mer, "Wear characterization of Al- Al_2O_3 in-situ particulate composite synthesized in open hearth furnace with manually controlled stirring method", Proceedings of international conference on innovation & research in technology for sustainable development (ICIRT), 2012.

[17] Agarwal, S. Singh and others, "Development of Al- Al_2O_3 (MnO_2) hybrid MMCs and their characterization for mechanical properties", MIT international journal of mechanical engineering, Vol. 2, No. 1, pp. 62-69, 2012.

[18] G. Kreysa, J. Baselt and K. Unger, Novel Mn-based Mesoporous mixed oxidic solids, Technology & Engineering, Elsevier, 2000.

[19] D Saheb, "Aluminum silicon carbide and aluminum graphite particulate composites", ARPN, Journal of engineering and applied sciences, Vol. 6, No. 10, ISSN 1819-6608, 2011.

[20] P. Sharma, "Production of AMC by stir casting – An overview", International journal of contemporary practices, ISSN: 2231-5608, Vol.2, Issue 1, 2013.

[21] R. Gadag and A. Shetty, Handbook of engineering chemistry, Department of chemistry, National institute of technology, Karnataka, Shurathkal, 2010.

[22] G. Totten and D. Scott, Handbook of aluminum, Physical metallurgy and processes, Vol. 1, 2003.

[23] J. Hashim, L. Looney and M. Hashmi, "The wettability of SiC particles by molten aluminum alloy", Journal of Materials Processing Technology, 119(1-3):324-328, 2001.

ISBN: 978-81-936820-6-7

Series: AIJR Proceedings
Proceedings DOI: 10.21467/proceedings.4